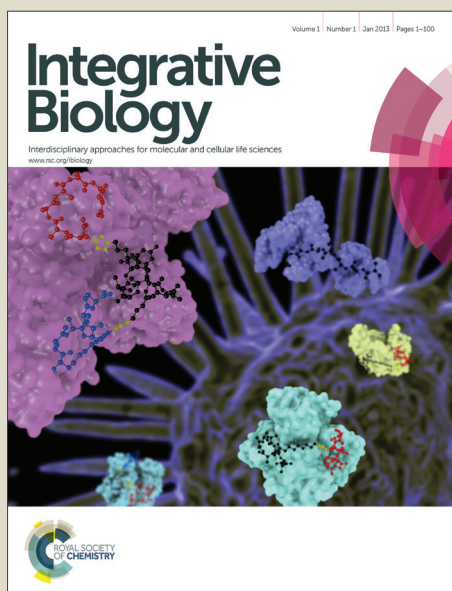


Integrative Biology

Accepted Manuscript



This is an *Accepted Manuscript*, which has been through the Royal Society of Chemistry peer review process and has been accepted for publication.

Accepted Manuscripts are published online shortly after acceptance, before technical editing, formatting and proof reading. Using this free service, authors can make their results available to the community, in citable form, before we publish the edited article. We will replace this *Accepted Manuscript* with the edited and formatted *Advance Article* as soon as it is available.

You can find more information about *Accepted Manuscripts* in the [Information for Authors](#).

Please note that technical editing may introduce minor changes to the text and/or graphics, which may alter content. The journal's standard [Terms & Conditions](#) and the [Ethical guidelines](#) still apply. In no event shall the Royal Society of Chemistry be held responsible for any errors or omissions in this *Accepted Manuscript* or any consequences arising from the use of any information it contains.

Table of contents

- 8 figures (+4 sup. Figures), no colour graphic
- One sentence highlighting the novelty of the work :
This study shows riboregulation by DsrA sRNA that binds mreB 5'-region to alter MreB levels and cell morphology during stresses
- Revised Electronic manuscript (word and pdf format)
- Response to the comments made by the reviewer

Insight, Innovation, Integration

The actin-like MreB protein determines the bacterial cell shape by directing cell-wall biosynthesis. In this paper we show that DsrA, a small noncoding RNA, is involved in the post-transcriptional regulation of *mreB* expression in *Escherichia coli*. Our quantitative analysis shed light on the interplay between transcriptional and post-transcriptional regulation of *mreB* in response to cellular stresses. In particular, to detect subtle morphological changes associated with this regulation, we used our experience in electron cryo-microscopy to obtain sharp measurements on frozen/hydrated *E. coli* K-12 whole cells, together with statistical analysis to unveil morphological differences in cell population. Our work provides, for the first time, an integrative analysis of *mreB* expression regulation during cellular stresses in the light of the associated alterations of cell morphology.

Riboregulation of the bacterial actin-homolog MreB by DsrA small noncoding RNA

Bastien Cayrol^{1,2}, Emilie Fortas^{1,2}, Claire Martret^{1,2}, Grzegorz Cech³, Anna Kloska³, Stephane Caulet^{1,2,4}, Marion Barbet^{1,2}, Sylvain Trépout^{5,6}, Sergio Marco^{5,6}, Aziz Taghbalout⁷, Florent Busi^{4,8}, Grzegorz Wegrzyn³ and Véronique Arluison^{1,2,4*}

¹ Laboratoire Léon Brillouin, CEA – Centre de Saclay, 91191 Gif-sur-Yvette, France

² UMR 12 CEA/CNRS, 91191 Gif-sur-Yvette, France

³ Department of Molecular Biology, University of Gdańsk, Gdańsk, Poland

⁴ Univ Paris Diderot, Sorbone Paris Cité, 75013 Paris, France

⁵ Institut Curie, Campus Universitaire d'Orsay, 91405 Orsay Cedex, France

⁶ INSERM U759, Campus Universitaire d'Orsay, 91405 Orsay Cedex, France

⁷ Department of Molecular Biology and Biophysics, University of Connecticut Health Center, 263 Farmington Avenue, Farmington, CT, 06032, USA

⁸ Unité de Biologie Fonctionnelle et Adaptative (BFA) UMR 8251 CNRS, 75205 Paris, France

* Corresponding author Veronique.Arluison@univ-paris-diderot.fr; Tel 33 1 69 08 32 82; Fax 33 1 69 08 95 36

Author contribution: BC, EF, CM, MB, SC, GC & AK performed most experiments. ST & SM designed and performed experiments, analyzed the data and wrote parts of the manuscript. FB, AT, GW & VA designed experiments, analyzed the data and wrote the manuscript.

Keywords: DsrA noncoding RNA, bacterial cell elongation, transcriptional and post-transcriptional regulation, σ^S , H-NS, peptidoglycan

Running title: *mreB* post-transcriptional regulation by a stress-related sRNA

SUMMARY

The bacterial actin-homolog MreB is a key player in bacterial cell-wall biosynthesis and is required for the maintenance of the rod-like morphology of *Escherichia coli*. However, how MreB cellular levels are adjusted to growth conditions is ill-understood. Here, we show that DsrA, an *E. coli* small noncoding RNA (sRNA), is involved in the post-transcriptional regulation of *mreB*. DsrA is required for the downregulation of MreB cellular concentration during environmentally induced slow growth-rates, mainly growth at low temperature and during stationary phase. DsrA interacts in an Hfq-dependent manner with the 5' region of *mreB* mRNA, which contains signals for translation initiation and thereby affects *mreB* translation and stability. Moreover, as DsrA is also involved in the regulation of two transcriptional regulators, σ^S and the nucleoid associated protein H-NS, which negatively regulate *mreB* transcription, it also indirectly contributes to *mreB* transcriptional down-regulation. By using quantitative analyses, our results evidence the complexity of this regulation and the tangled interplay between transcriptional and post-transcriptional control. As transcription factors and sRNA-mediated post-transcriptional regulators use different timescales, we propose that the sRNA pathway helps to adapt to changes in temperature, but also indirectly mediates long-term regulation of MreB concentration. The tight regulation and fine-tuning of *mreB* gene expression in response to cellular stresses is discussed in regards to the effect of the MreB protein on cell elongation.

Abbreviations: Cryo-TEM: cryo-transmission electron microscopy; EtBr: ethidium bromide; nt: nucleotide; PAGE: polyacrylamide gel electrophoresis; PG: peptidoglycan; rbs: ribosome binding site; RT-qPCR: reverse transcription quantitative PCR ; sRNA: small regulatory noncoding RNA

Introduction

Small regulatory noncoding RNAs (sRNA) range from ~ 40 to 400 nucleotides and are used by bacteria as environmental response actors (for recent reviews see references ¹⁻³). Most of these RNAs are trans-encoded and transcribed under cellular stresses. They act by an antisense mechanism *via* base-pairing to their target mRNA to form imperfect short duplexes that require the RNA chaperone Hfq protein for their stabilization and proper function in Gram negative bacteria.^{4, 5} mRNA-sRNA interactions usually take place in the vicinity of the ribosome binding site (rbs) and thereby modulate translation efficiency and mRNA stability, for instance by exposing a cleavage site for RNaseE.³ One of the best-characterized *Escherichia coli* sRNA is DsrA, an 87 nucleotide RNA encoded by a gene located in the downstream region of *rcaA*, which encodes a transcriptional activator of polysaccharide capsule synthesis genes.⁶ DsrA was shown to sense environmental changes through its inherent temperature-sensitive transcription initiation and to stimulate the expression of the major stress regulator sigma factor σ^S .⁷ *rpoS* mRNA (encoding σ^S) usually forms a secondary structure within its 5'-untranslated region, which results in poor translation due to weak ribosome accessibility to the rbs. Nevertheless, efficient *rpoS* translation takes place upon disruption of the secondary structure within the 5' regulatory region by the Hfq-mediated DsrA-binding to an upstream sequence in the 5'-untranslated leader region of *rpoS* mRNA.⁸⁻¹⁰ Hence, transcription of σ^S -dependent genes is induced at low temperature in exponential phase and during stationary phase, a process that permits the cell to adapt to these stresses.¹¹⁻¹⁴

Many sRNAs have multiple targets and can therefore affect the translation of multiple mRNAs to coordinate or synchronize different cellular pathways. For example, DsrA binds to both *hns* and

rpoS mRNAs and thus influences the expression of two global transcriptional regulators, leading to a reduction in cellular levels of the H-NS histone-like nucleoid structuring protein and to an accumulation of σ^S .^{6, 15} Thus by acting on transcription factors, these sRNA-based regulation pathways result in important effects at the transcriptional level.¹⁶ In addition, the regulation of a specific mRNA by multiple sRNAs can also occur. For instance, at least four different sRNAs (DsrA, OxyS, RprA and ArcZ) have been shown to control *rpoS* expression under different environmental stresses.^{17, 18}

As many sRNAs accumulate during the stationary phase of growth when bacteria stop dividing¹⁹, it was proposed that sRNAs could influence the expression of genes coding for cell division proteins.²⁰ For example, the tubulin-like FtsZ that directs formation of the cytokinetic ring²¹ is thought to be regulated at the translational level by the DicF sRNA in a process that requires Hfq.^{20, 22, 23} Similarly, an Hfq-dependent negative post-transcriptional regulation of the actin-homolog MreB was previously reported but the putative sRNA(s) involved in the process was not identified.²⁰

MreB plays an essential role in maintaining the rod shape of *E. coli*.²⁴⁻²⁶ Current models propose that MreB forms membrane-associated patches²⁷, helps to organize the membrane in domains²⁸ and that together with the transmembrane proteins MreC, MreD or RodA, plays an important role in the peptidoglycan synthesis required for cell shape maintenance (for recent reviews see references^{26, 29}). The interplay between MreB and the enzymes producing peptidoglycan helps to maintain the bacterial cell shape. When MreB concentration declines or when its polymerization is inhibited, the cell loses its rod shape and becomes round like cocci that naturally lack MreB.³⁰ How *mreB* gene expression is regulated is not well understood. Three σ^{70} -dependent promoters contribute to *mreB* expression in *E. coli* (Sup Fig. S1).³¹ The *mreB* gene, in many bacteria, is

found in the same operon as *mreC* and *mreD* genes, which code for proteins required for coordinating peptidoglycan insertion.³¹ Most *mreB* transcripts of the *mre* operon are monocistronic, while polycistronic *mreBCD* mRNA seems to be scarce.³¹ Under stress response, BolA, whose expression is driven by the σ^S factor, binds *mreB* promoters and represses *mreB* transcription.³²⁻³⁴ This indicates that stresses, including entry into the stationary phase, lead to a reduced MreB protein level.³⁴

In this study, we identify a newly discovered pathway of post-transcriptional regulation of MreB cellular levels, where Hfq-mediated interaction of the stress-induced DsrA with *mreB* transcript interferes with *mreB* expression. We propose a model for *mreB* gene regulation in which DsrA acts directly as an antisense sRNA to down-regulate the *mreB* mRNA translation and stability. Furthermore, DsrA is able to indirectly influence σ^S and H-NS-dependent inhibition of *mreB* transcription. We discuss here how this regulation affects the elongation of dividing *E. coli* cells.

Results

Hfq and DsrA downregulate the expression of mreB

DsrA, an *E. coli* sRNA, was previously shown to be transcribed under natural environmental changes. DsrA concentration increases when temperature drops off and during stationary phase.^{7, 13, 35} Because we observed reduced MreB levels in cells grown at low temperature and during stationary phase, we sought to determine the role of induced *dsrA* expression on MreB protein levels. We first performed quantitative Western Blot analyses of MreB on total protein extracts from wild-type cells and mutants that lacked DsrA or Hfq. This was tested in wild-type strains, and in *dsrA* or *hfq* mutants, since Hfq is a known cofactor for DsrA. This showed, and consistent

with a previous report²⁰, that growth at low temperature or stationary phase are associated with decreased levels of MreB in wild-type cells (Fig. 1, WT columns). Exponentially growing cells showed normal concentration of MreB at 37°C regardless of the presence DsrA or Hfq. In contrast, at 16°C and during stationary phase, cells that lacked either DsrA or Hfq showed 30 to 50% more MreB than the respective wild-type cells (Fig. 1), suggesting that DsrA was responsible for part (stationary phase) or all (16°C) of the decline.

Because the observed decrease in cellular MreB could result from other effects of cold or stationary phase-associated stress signals not necessarily mediated by *dsrA* expression, we tested the effect of heterologous expression of *dsrA* on MreB levels. The expression of *dsrA* in wild-type cells at 37°C from either an arabinose inducible (P_{BAD}) or a constitutive ($P_{LlacO-1}$) promoters showed decrease in MreB levels (Sup Fig. S2). The fact that down-regulation of MreB levels was obtained strongly suggests that expression of *dsrA* leads to reduced MreB levels independently of other cellular stresses. Furthermore, the expression of the *dsrA* gene in $\Delta dsrA$ cells from arabinose inducible promoter at 16°C resulted in similar decrease in MreB concentration as seen in wild-type cells grown at 16°C (Fig. 1). The *dsrA* gene expression from P_{BAD} arabinose induced promoter was carried out under conditions that give an *rpoS-lacZ* fusion activity comparable to that seen from the single-copy chromosomal *dsrA*.⁸

To test the effect of cold-induced *dsrA* expression on *mreB* transcription, we used plasmid born *mreB-lacZ* transcriptional fusions where one or more *mreB* promoters (P_{mreB}^1 , P_{mreB}^2 & P_{mreB}^3), and the native ribosome binding site and start codon (AUG) were fused to *lacZ* coding region (see Sup Fig. S1).³⁶ As previously reported, the transcription activity from the *mreB* promoter was reduced to approximately 50 % in the absence of P_{mreB}^3 or P_{mreB}^2 and P_{mreB}^3 , as indicated by β -galactosidase assays (Sup Fig. S3, columns 1, 6 and 10).³⁶ Interestingly, the effects of cold-

induced expression of *dsrA* at 16°C on *mreB* expression were within 10-20%, independently of the presence of one or more *mreB* promoters (P_{mreB}) (Sup Fig. S3, compare columns 1-2, 6-7 and 10-11). Furthermore, expression of *dsrA* under the control of inducible promoter in $\Delta dsrA$ cells gave similar results as WT cells (Fig. S3, compare columns 1-3, 6-8 and 10-12). This indicates that *dsrA* expression down regulates *mreB* expression and that the region containing P_{mreB}^2 and P_{mreB}^3 does not have a major effect for the observed DsrA-mediated effect on *mreB* expression *in vivo*.

To establish whether the predicted DsrA regulation affects *mreB* mRNA translation, we used an in-frame translational *mreB-lacZ* reporter fusion expressed under the control of P_{BAD} inducible promoter in wild-type cells and mutants that lacked DsrA or Hfq. The cellular levels of the MreB-LacZ protein would therefore be altered only by post-transcriptional regulatory event(s). The *mreB-LacZ* fusion includes only P_{mreB}^1 transcription initiation site as DsrA mediated down regulation of *mreB* expression was independent of P_{mreB}^2 and P_{mreB}^3 (see sup Figs. S1, S3). This showed, similarly to the quantitative immunoblot of MreB (Fig. 1), no significant changes in MreB levels in $\Delta dsrA$ cells growing exponentially at 37°C as indicated by the β -galactosidase levels (Fig. 2). However, at low temperature or in stationary phase, when DsrA is efficiently produced in wild-type cells, deletion of *dsrA* increased expression of the translational fusion by a factor 2 or 1.7, respectively (Fig. 2). The lack of Hfq resulted in a significant increase of *mreB-lacZ* mRNA translation in cells grown under normal and stress conditions, suggesting a possible additional negative effect of Hfq on *mreB-lacZ* mRNA stability and/or translation independently of DsrA. Although the expression of the fusion was significantly reduced during stationary phase, the lack of DsrA or Hfq resulted in the same trend and led also to a significant increase of the *mreB-lacZ* expression. A possible reason for low activity during stationary phase could be

due to generally less efficient anabolic processes in bacteria in stationary phase, thus experiencing nutritional limitations. However, the low activity was not due to consumption of inducer as arabinose was added to harvested stationary phase cells.

DsrA regulates the expression of *mreB* through direct base pairing interaction

Evidence that DsrA, as small noncoding RNA, could interfere with *mreB* expression through direct base pairing with *mreB* mRNA came from RNA duplex prediction obtained by using RNAfold web server.³⁷ This showed a predicted model for DsrA:*mreB* RNA duplex structure where DsrA interacts with site of *mreB* mRNA that includes *mreB* translation initiation codon (Fig. 3), suggesting that DsrA-binding could strongly interfere with initiation of *mreB* mRNA translation. This model supports the conclusion drawn from DsrA-mediated reduction of β -galactosidase activity in the *mreB-lacZ* fusions.

To test this model for direct *mreB*:DsrA annealing, we asked whether the DsrA-mediated regulation of MreB levels is affected by mutations in *dsrA* that alter *mreB*-DsrA annealing and by mutations in *mreB* that restore annealing to the mutant DsrA (Sup. Fig. S4). We thus compared β -galactosidase activity in $\Delta dsrA$ cells that expressed a combination of plasmid encoded *mreB-lacZ* fusion and/or *dsrA* allele under the control of P_{BAD} promoters at 37°C. As shown in Fig. 4, expression of *mreB^{WT}-lacZ* was significantly reduced upon transcription of *dsrA^{WT}* (repression of 90 %), while the mutant derivative of DsrA where the region involved in the predicted annealing with *mreB* mRNA was mutated (DsrA^{mut}) did not affect the β -galactosidase activity from *mreB^{WT}-lacZ* fusion (repression of 9 %, Fig. 4). Similarly, when *mreB-lacZ* fusion carrying compensatory mutation that restores annealing with DsrA^{mut} was expressed, DsrA^{WT} failed to alter *mreB^{mut}-lacZ* expression whereas DsrA^{mut} restored repression

(repression of 70 %). Together, these results clearly show that DsrA basepairs with *mreB* mRNA around *mreB* start codon and affects MreB expression, confirming the direct annealing model presented on Fig. 3. The annealing could directly interfere with *mreB* translation by limiting ribosome access to the translation site. However, DsrA could also interfere with the *mreB* gene expression by altering *mreB* mRNA stability.

DsrA affects the cellular concentration of *mreB* mRNA

To determine whether DsrA affects *mreB* mRNA cellular levels, we performed absolute quantifications of DsrA and *mreB* RNAs by using a reverse transcription quantitative-PCR (RT-qPCR) assay in wild-type cells and mutants that lacked DsrA or Hfq, as previously described.³⁵ This showed in wild-type cells that DsrA was present at 4 copies per cell at 37°C and that DsrA level increased to 10 copies per cell at 16°C (Fig. 5). These results slightly differ from absolute measurements made in the MC4100 strain³⁵, but are nevertheless in agreement with those reported previously.^{7, 13, 35, 38} Consistent with a previous report, we also found that DsrA produced due to activity of the chromosomal gene is nearly absent in cells lacking Hfq, probably because of DsrA instability in the absence the Hfq protein.^{35, 39}

Measurements of cellular mRNA levels showed that the *mreB* mRNA was present at 9 copies per exponentially growing WT cell at 37°C (Fig. 5), a level which decreased to less than 5 copies per cell at low temperature (16°C), suggesting that DsrA negatively influences *mreB* mRNA concentration. However, cells that lacked DsrA only showed a moderate increase in *mreB* mRNA cellular abundance at low temperature (~20% increase).

During stationary phase, *mreB* mRNA cellular concentration was greatly reduced as it reached less than one copy per cell. This could reflect a cumulative effect of *drsA* expression and changes

in *mreB* transcription during the stationary phase of growth (see Discussion). However, the lack of DsrA resulted in an increase of *mreB* mRNA abundance during stationary phase (Fig. 5).

As *mreB* mRNA stability could be affected during cellular stress, we measured *mreB* mRNA half-life during growth at low temperature. For stationary phase, *mreB* mRNA abundance was too low to accurately estimate its half-life (Fig. 5). As shown in Fig. 6, expression of DsrA at low temperature significantly destabilized the *mreB* transcript as indicated by the 40% decrease of its half-life in WT cells at low temperature. Thus, *mreB* mRNA was greatly destabilized when DsrA was induced at 16°C and was significantly stabilized in cells that lacked DsrA.

The absence of Hfq resulted in less *mreB* transcript under normal exponential growth conditions when compared to wild-type cells (Fig. 5). This was consistent with the increased degradation rate of *mreB* mRNA as shown by the change of its half-life from 3.15 min in the WT to 1.21 min in the *hfq* mutant (Fig. 6), thus suggesting a DsrA-independent effect of the RNA chaperone Hfq that stabilizes *mreB* mRNA under exponential growth conditions at 37°C. Indeed, it is likely that Hfq protects *mreB* transcript against RNaseE due to the overlapping cleavage sites and Hfq binding sites on the mRNA.⁴⁰ Conversely, during exponential growth at 16°C where the riboregulation by DsrA occurs, the absence of Hfq resulted in a completely different effect. *mreB* mRNA stability was greatly increased in cells that lacked DsrA or Hfq (Fig. 6). This result confirms that Hfq is required for the DsrA-mediated riboregulation during stress as the absence of Hfq, which enables the sRNA to anneal with its target, results in a stabilization of the mRNA. However, the lack of Hfq produced a significantly greater stabilization of *mreB* mRNA than the absence of DsrA, suggesting a role of other unidentified Hfq-dependent sRNAs. *mreB* mRNA destabilization might be mediated by an RNaseE-Hfq ribonucleoprotein complex as is the case of SgrS and RyhB sRNAs^{1,41} or a passive mechanism due to abortive translation.⁴²

Stress regulation by DsrA influences the elongation of dividing cells

We showed that DsrA mediates posttranscriptional down-regulation of *mreB* expression, leading to a 30 % reduction in cellular MreB (Fig. 1, WT-exponential phase 37°C vs 16°C). MreB is required for maintenance of the bacterial rod-shape as cells that lose MreB shorten and become round-shaped.²⁶ We therefore investigated whether DsrA-mediated regulation of *mreB* expression is associated with morphological changes of the cells. We used high-resolution microscopy cryo-TEM technique to measure cell length (L) and width (w) for a population of about 50 cells in wild-type, and $\Delta dsrA$ cells and in each condition we determined the cell roundness as calculated from the cellular width to length ratio (w/L). The rod-shaped *E. coli* cell is approximately 1.5 μm long and 0.7 μm wide (roundness ~ 0.47). As shown in Fig. 7, exponentially growing WT cells (DJ480) at 37°C showed two cellular populations: one rod-shaped (~ 70 %) with a roundness of ~ 0.36 ($\sigma^2=0.05$) and the other short (~ 30 %) with a roundness of ~ 0.48 ($\sigma^2=0.05$). Intuitively, we can assume that the short population represents new-born cells whereas long rod population corresponds to cells that had elongated but did not divide. Similarly, exponentially growing WT cells at 16°C (in which MreB level is decreased by ~ 30 %, see Fig. 1) also showed rod-shaped and short populations with a roundness of ~ 0.37 ($\sigma^2=0.05$) and 0.49 ($\sigma^2=0.05$), respectively. However, the short population is slightly more abundant than at 37°C, a result in agreement with reduced MreB levels observed by Western Blot that should affect elongation of dividing cells. Conversely, cells that lacked DsrA (NM317) especially at 16°C clearly showed mostly one population with a roundness of 0.45 ($\sigma^2=0.01$) at 16°C and 0.42 ($\sigma^2=0.01$) at 37°C. This result indicates that in the absence of DsrA, cells remain longer and more rod-shaped. Further evidence for the role of DsrA riboregulation of *mreB*

expression in affecting cellular morphology came from complementation assays of $\Delta dsrA$ cells. Synthesis of plasmid-encoded DsrA (pNM13) was induced in $\Delta dsrA$ cells by using an arabinose concentration that gave an *rpoS-lacZ* fusion activity comparable to that seen from the single-copy chromosomal *dsrA*.⁸ The *dsrA* expression restored two cellular populations with roundness of 0.33 ($\sigma^2=0.01$) and 0.48 ($\sigma^2=0.01$) (Fig. 7) and is consistent with Western Blot analysis (Fig. 1) and *mreB-lacZ* expression (Fig. S3), which showed *mreB* expression at levels similar to that found in cells in the absence of stress.

During stationary phase, both WT (DJ480) and $\Delta dsrA$ (NM317) strains form rounder cells. However $\Delta dsrA$ cells were less round than WT cells (roundness of 0.50 ($\sigma^2=0.01$) vs 0.59 ($\sigma^2=0.01$)). This suggests that, in addition to DsrA riboregulation, other mechanisms affect cell morphology during stationary phase.

In all, these results confirm that *mreB* expression regulation by DsrA affects the elongation of dividing *E. coli* cells during growth at low temperature and stationary phase.

Because the observed difference in cell morphology could be due to a growth defect in $\Delta dsrA$ cells, we therefore compared the growth of wild type and $\Delta dsrA$ mutant at low temperature. This showed that the doubling times were 33 and 32 min at 37°C, and were 300 and 270 min at 16°C for wild type and $\Delta dsrA$ mutant, respectively. Consistent with previous reports, the growth rates did not change significantly for the mutant and the wild type strains at either temperature.^{13, 14}

Discussion

In this work we studied how DsrA, a small noncoding RNA, regulates the expression of *mreB* gene during growth at low temperature and stationary phase and how the regulation affects the

morphology of dividing *E. coli* cell (see Table 4 for a summary). Small regulatory RNAs and transcription factors are two means used by the bacterial cell for regulation of gene expression.⁴³ *mreB* was previously shown to be negatively regulated at the transcriptional level by the BOLA transcription factor, which interacts with the *mreB* promoter and alters *mreB* transcription mainly during stationary phase.³⁴ Transcription of the *bolA* gene is driven by the σ^S factor.^{44, 45} Although all sRNAs involved in *rpoS* riboregulation during stationary phase have not been identified, positive regulation by sRNAs indeed results in an increase in BOLA concentration, leading to a significant reduction of *mreB* transcription and consequently in MreB protein level (Fig. 8), which causes rounder morphology.^{34, 45}

Furthermore, *bolA* transcription is directly repressed by the global regulator and DNA organizer H-NS, which itself is downregulated by DsrA sRNA (Fig. 8).^{15, 46} Indeed, as shown on figure 5, we observed that in $\Delta dsrA$ strain, growth at low temperature resulted in a modest increase of *mreB* mRNA concentration (20% more relative to WT strain). Nevertheless, we also observed that during stationary phase, *mreB* concentrations are very low. The fact that DsrA concentration is only slightly increased during this phase of growth (see Fig. 5)³⁵ suggests that other sRNAs might play an important role in σ^S production and consequently in *bolA* transcription.^{17, 18}

We show that *mreB* expression is negatively regulated at the post-transcriptional level by the stress-related noncoding small RNA DsrA, which is involved in *rpoS* and *hns* transcription regulation (Fig. 8). We also showed that DsrA regulates the expression of *mreB* through an Hfq-assisted base pairing that presumably prevents ribosome binding. A similar mechanism was shown for several negatively acting sRNAs.⁴⁷ Consistent with this, we showed that *mreB* translational regulation is abolished in the absence of DsrA sRNA or Hfq. We also showed that DsrA and Hfq influence *mreB* mRNA concentration and turnover, suggesting a role for DsrA

and Hfq in the control of *mreB* mRNA stability. However, the increase in *mreB* mRNA concentration associated with the absence of DsrA can result from both BolA-mediated *mreB* transcriptional regulation via σ^S and H-NS³⁴ and changes in *mreB* mRNA stability (Fig. 8). The fact that DsrA regulation was observed with *mreB-lacZ* fusions whose expression is independent of BolA clearly shows that the observed DsrA-mediated down regulation of MreB synthesis includes a direct effect of DsrA on *mreB* translation and stability (Figs. 2 and 4).

This second point of control for MreB synthesis, which occurs subsidiarily to transcriptional control, is probably required for the cell as MreB is an abundant protein (in average ~10 000 copies/cell).⁴⁸ Nevertheless, MreB protein abundance is not necessarily correlated to the cellular concentration of its mRNA. If *mreB* mRNA is abundant as MreB, its translation and/or stability would unlikely be efficiently regulated by a sRNA of low abundance such as DsrA. Here we measured for the first time *mreB* mRNAs steady-state level and showed that *mreB* mRNA is indeed present at a maximum of 9 copies per cell, a result in agreement with a possible regulation by DsrA. The copy number of *mreB* mRNA could appear too low for an abundant protein. Nevertheless, mRNA steady state copy number only reflects recent transcription events and can usually not be correlated with the protein concentration, which has a longer lifetime than the bacterial cell cycle and represent accumulated transcriptions.⁴⁹ In *mreB* case, to have $n_m=9$ mRNA copies per cell implies that the cell needs a transcription rate of $9 \times \delta_m$, where δ_m is *mreB* mRNA degradation rate (m for *mreB* mRNA). As the degradation rate is the sum of active degradation by RNases and dilution by cell growth, the degradation rate $\delta_m = \ln 2/\tau_{hl-RNA} + \ln 2/\tau_{cc-RNA}$ where τ_{hl-RNA} is the mRNA half-life (3.15 min) and τ_{cc-RNA} is the cell doubling time (30 min). This indicates that the cell needs to produce ~ 2.2 mRNA molecules per minute or ~ 70 per doubling time. Protein number in steady state is $N_m = [(\beta_m \times n_m) / \delta_m]$, where β_m is *mreB* mRNA

translation rate, n_m is *mreB* mRNA copy number and δM is the MreB protein degradation rate (M for MreB protein); protein degradation rate $\delta_M = \ln 2 / \tau_{hl-prot} + \ln 2 / \tau_{cc-prot}$. Since MreB protein is probably stable, protein degradation rate is $\delta_M = \ln 2 / \tau_{cc-prot}$. In steady state, MreB protein is present at $\sim 10\,000$ copies per cell and we measured that the number of mRNA copies is ~ 9 , so translation rate is ~ 25 protein copies per mRNA per minute. Since *mreB* mRNA mean life-time ($1/k$) is 4.5 min and translation rate is 25 copies per mRNA per minute, one *mreB* mRNA is translated on average 110 times before being degraded. This is in agreement with the estimated range of 1-150 translation events per mRNA in *E. coli*⁴⁹ and with what should be expected for an efficiently produced protein such as MreB.

The relative contribution of these transcriptional and post-transcriptional regulatory pathways remains to be determined. Intuitively, we might expect that sRNA regulation would allow the reduction of the delay to turn off *mreB* expression relative to the use of protein-based transcription control, although sRNA regulation can also introduce intrinsic noise.^{35, 43, 50, 51} In addition, due to the high stability of DsrA in WT cells whose half-life was estimated to 23 min at 25°C in a previous work³⁸, this sRNA pathway is probably cost-effective for the bacterial cell, as the energy required to synthesize a sRNA is small compared with the energetic cost needed for the synthesis and translation of a mRNA. Note that steady state and half-life measurements of *mreB* mRNA could differ for a specific condition; for instance, at 16°C, *mreB* mRNA half-life increases by a factor 10 in an *hfq* mutant compared to wild-type (Fig. 6), while steady state mRNA levels are slightly lower in the *hfq* mutant compared to those found in wild-type (3.5 copies/cell compared to 4.5 copies for WT, Fig. 5). This indeed reasserts that steady state measurements do not only result from the efficiency of RNA degradation but also from an intricate interplay with transcription. As we can see, the absence of Hfq greatly increases *mreB*

mRNA stability whereas, as a pleiotropic regulator, it likely affects transcription independently of DsrA.^{52, 53}

Experimentals

Chemicals, reagents, and oligodeoxyribonucleotides

All chemicals and reagents were purchased from Sigma-Aldrich or Thermo Fisher Scientific unless otherwise specified. Oligonucleotides were purchased from Eurogentec (Belgium).

E. coli strains, plasmids and growth conditions

Bacterial strains and plasmids used in this study are shown in Table 1. The *hfq::kan* or *hfq::cm* alleles^{54 55} (when necessary for the compatibility with plasmids) were moved in appropriate genetic backgrounds by P1 transduction. For long-term growth at low temperature condition, cells were grown at 16°C and then induced by L-arabinose at the same temperature when indicated. For stationary phase conditions, cells were grown at 37°C overnight. L-arabinose concentrations used in the various experiments are indicated in the corresponding experiments.

Constructions of pNM13, a derivative of pBAD24 (ColE1, Amp^R)⁵⁶ mutated to generate a promoter-less *dsrA* DNA fragment under the control of the arabinose promoter P_{BAD}, and the corresponding empty plasmid (pNM12), were previously described.⁸ pNM12 serves as a control for exposure to L-arabinose and antibiotic.

For the construction of pZE12-DsrA (ColE1, Amp^R), a *dsrA* PCR fragment was ligated into the pZE12 plasmid under the control of the constitutive P_{LacO-1} promoter.⁵⁷ When necessary, ampicillin resistance was replaced by kanamycin in order to allow co-transformation with other

plasmids. For the construction of pBAD33-DsrA, a *dsrA* PCR fragment was inserted into pBAD33 (p15A, Cm^R) under the control of the P_{BAD} promoter.⁵⁶ Construction of the pMEC1 series (pSC101, Kan^R) was previously described.³¹ Note that *mreB*, *mreC* and *mreD* genes form an operon and that pMEC1 series allow the expression of the three proteins from the respective 3 promoters P_{mreB}¹, P_{mreB}² and P_{mreB}³ for pMEC1, from P_{mreB}¹ and P_{mreB}² for pMEC1s and from P_{mreB}¹ only for pMEC1ss (Sup Fig. S1).³¹ For the construction of pNM12mreB-lacZ, a PCR product carrying -43 to +495 nts of *mreB* relative to its Start codon was amplified from genomic DNA (MG1655) using the Phusion polymerase and primers carrying homologies to P_{BAD} promoter and *lacZ*. *lacZ* was amplified from pMEC1. *mreB* and *lacZ* PCR fragments were assembled by PCR and inserted into the pBAD24 derivative pNM12.⁸

β-Galactosidase assays

Overnight cultures of cells-containing plasmids were diluted into fresh LB (supplemented with glucose and ampicillin, chloramphenicol or kanamycin as indicated), grown at the indicated temperature and harvested at OD₆₀₀ = 0.3 for exponential phase analyses. For stationary phase analyses, overnight cultures are used. Expression of the *lacZ* fusions was induced by the addition L-arabinose. To remove glucose before induction, the culture was spun down and resuspended in LB containing glycerol (0.2 %) and L-arabinose for 1 hour (concentration of L-arabinose is indicated in the legend of corresponding figures). β-galactosidase activity was assayed using 0.1 ml culture as described in Miller.⁵⁸ The β-galactosidase activities are the average value of at least three independent experiments.

Construction of complementary mutations

As pNM13 and pNM12*mreB-lacZ* are incompatible plasmids, we used for this analysis the pNM12*mreB-lacZ* plasmid (ColE1, Amp^R) and DsrA was expressed from pBAD33 (p15A, Cm^R). The following sequences have been used for WT and complementary mutations (the mutated region is underlined)

DsrA^{WT}:

5'ACACAUCAGAUUCCUGGUGUAACGAAUUUUUUAAGUGCUUCUUGCUUAAGCA
AGUUUCAUCCCGACCCCCUCAGGGUCGGGAUUU3'

DsrA^{mut}:

5'ACACAUCAGAUUCCUGGUGUUUGCUUAAAAAAGUUGCUUCUUGCUUAAGCA
AGUUUCAUCCCGACCCCCUCAGGGUCGGGAUUU3'

mreB^{WT} (AUG codon is indicated in bold):

5'...UUAGUA**AUG**UUGAAAAAAUUUCGUGGCAUGUUUUCCAAUGACUUGU... 3'

mreB^{mut}: (Note that we conserve the in frame translation for *mreB*^{mut}-*lacZ* sequence)

5'...UUAGUA**AUG**AAUUUUUUUAAAGCAGGCAUGUUUUCCAAUGACUUGU... 3'

Mutant RNAs annealing was confirmed with the RNAfold web server (Sup Fig. S4).³⁷

Changes in DNA sequence of *dsrA* and *mreB* were introduced using PCR-based site-directed mutagenesis using FastStart High Fidelity PCR System (Roche) with 1.25 pmol of appropriate primers listed in Table 3 and 50 ng of pBAD33-DsrA or pNM12*mreB-lacZ* vectors as template in 12.5 µl reaction volumes. PCR conditions were as follows: denaturation at 95°C for 5 min; 18 cycles of 95°C for 50 sec, 50°C for 50 sec and 68°C for 1 min per each 1 kb of template DNA + additional 1 min; final extension at 68°C for 7 min. PCR products were subjected to *DpnI* digestion at 37°C for 1 hour to eliminate the template DNA and then used for bacterial

transformation of DJ480 competent cells. Resulting plasmids, pBAD33-DsrA^{mut} and pNM12*mreB*^{mut}-*lacZ*, are listed in Table 1.

RNA extraction, reverse transcription and RT-qPCR analysis

Total RNA preparation, reverse transcription and RT-qPCR analysis were performed as described previously.³⁵ Briefly, 3 pmol of a fragment of *kan* transcript fragment (103 nt, T7 *in vitro* transcription) was added to the bacterial lysate prior to RNA extraction to normalize quantitation. RNAs were then extracted by hot-phenol and ethanol precipitated from cell lysate made from 20 ml cultures grown to OD₆₀₀ 0.6. Samples were subjected to a RQ1 DNase treatment (RNase-free) for 1 hour at 37°C followed by phenol/chloroform extraction. The cDNA synthesis was performed at 37°C using the M-MuLV RT (Fermentas) and the indicated reverse primer (Eurogentec) and incubating at 37°C for 60 min followed by 5 min at 85°C to inactivate the reverse-transcriptase. Negative controls were incubated in the absence of reverse transcriptase.

Quantification of transcript was performed by real time RT-qPCR using a LightCycler® 480 instrument (Roche) and a SYBR Green I based method as described previously.³⁵ Four sequences were amplified: *dsrA*, *mreB*, *kan* and *rrsB*. *rrsB* housekeeping gene was used to normalize RNA quantity in each reaction and *kan* to calculate the efficiency of RNA extraction. The primers used for amplification are shown in Table 2.

Western Blot analysis

E. coli cells pellets were re-suspended in TE buffer containing 4% w/v SDS and 10% v/v β-mercaptoethanol and boiled 95°C for 5 min. Equal amounts of total protein were loaded on 10%

SDS-PAGE gels. After a transfer at 4°C on a nitrocellulose membrane using a mini-protean transfer blot module (Bio-Rad), blocking step was done in 5% Defatted Milk in PBS 1X containing 0.1% tween 20. Membranes were then successively incubated with purified rabbit anti-MreB antibody⁵⁹, secondary anti-rabbit HRP conjugated antibody (GE Healthcare) and revealed with ECL Western Blot substrates (Pierce) using a G-box imager (SynGene). Intensities of bands were evaluated using the ImageJ software.⁶⁰ For accurate measurement, the protein concentrations were chosen where linear relationship existed between the protein concentration and the immunostaining intensity. The assay was repeated for 3 independent extracts in each condition. *ΔmreBCD* strain was used as negative control.

mRNA stability assay

E. coli strains were grown at 37°C and 16°C to exponential phase. Stationary phase cells were grown at 37°C. Rifampicin was added at 200 µg/ml to stop transcription and then samples were taken at several time points after rifampicin addition (time ranging between 0 and 60 min). Each sample was chilled on ice in the presence of 30 mM sodium azide and then total RNAs were extracted using High Pure RNA Isolation Kit (Roche) according to the manufacturer's instructions, which include DNase I treatment of the samples. The total concentration of RNA was measured. Finally, reverse transcription was performed using Thermo Scientific RevertAid H minus Reverse Transcriptase and specific primers, according to manufacturer's instructions. The relative quantification of transcript was performed by real time RT-qPCR. Normalization was performed by using the amount of total RNA in each RT reaction (250 ng) and by the level of expression of a reference gene (*rrsB*) at time zero point (before addition of rifampicin). Relative mRNA level in each sample was normalized to time zero point for each strain. The half-

lives of transcripts were estimated after curve fitting of the kinetics with an exponential decay model ($A = A_0 \cdot \exp(-k \cdot t) + B$).

Cryo-Transmission Electron Microscopy (cryo-TEM)

Cells grown at 16°C or 37°C were prepared for cryo-transmission electron microscopy as described previously.⁶¹ Z-loss images (25eV slit) of each sample were recorded on a JEOL 2200FS cryo-transmission electron microscope operated at 200 kV by using a Gatan 2kx2k Ultascan ssCCD camera at average defocus and nominal magnification of -10 μm and 5000x respectively. Length and width of bacteria were measured using ImageJ software (<http://rsb.info.nih.gov/ij/>)⁶² to determine their roundness defined as the ratio between the minimal and the maximal axes of each cell. Populations in each condition were analyzed by using the Mixtool package⁶³, to examine multimodal distributions by Gaussian fitting determining the average size and their associated variances (σ^2) in different experimental conditions.

RNA secondary structure modeling

RNA secondary structure models were predicted by the RNAfold web server (<http://rna.tbi.univie.ac.at/cgi-bin/RNAfold.cgi>) with default options.³⁷

Conclusion

Taken together, our data suggest that at least two riboregulatory pathways are involved and coordinated for *mreB* expression: direct post-transcriptional regulation by DsrA, which occurs via DsrA/*mreB* pathway, whereas indirect transcriptional regulation takes place via the

DsrA/ σ^S /BolA/H-NS pathways (Fig. 8). Although deletion of DsrA does not appear to impact growth rate at low-temperature and is not detrimental under laboratory conditions, DsrA might nevertheless be important in natural environments where bacteria live under combination of stresses that could make sRNA-mediated *mreB* regulation important for cell elongation and survival.

Furthermore, taking into account the evolutionary conservation of DsrA in many bacteria⁸, this regulatory mechanism might also apply to other bacterial species other than *E. coli*. Indeed morphological changes associated with *mreB* regulation during various stresses has been reported in *Vibrio parahaemolyticus*.⁶⁴ Nevertheless, whether an sRNA mediates the regulation in this bacterium is not known.

Acknowledgements

We are grateful to N. Majdalani, S. Gottesman (NIH, Bethesda, MD) and M. Wachi (Tokyo Institute of Technology, Japan) for providing strains and plasmids. We are indebted to D. Joseleau-Petit (Université Paris Diderot, Paris, France) who contributed to this work at an early stage, to P.J. Choi (Harvard Medical School, Boston, MA) and R. Guantes (Universidad Autónoma de Madrid, Spain) for many fruitful discussions. We thank PICT-Ibisa for providing access to JEOL 2200FS cryo-TEM. We are finally indebted to L. Rothfield (University of Connecticut Health Center, USA), J. Voss (University of Cambridge, UK), N. Figueroa-Bossi and L. Bossi (CGM/CNRS, Gif sur Yvette, France) for their critical reading of the manuscript.

Funding

This work was supported by FP7 DIVINOCELL Health-F3-2009-223431, PHC Polonium N° 27701VG, University Paris Diderot, CNRS and CEA (VA), National Science Center Poland grant no. 2012/04/M/NZ1/00067 (GW) and by NIH grant R37 GM060632 (AT).

Disclosure of Potential Conflicts of Interest

No potential conflicts of interest were disclosed.

References

1. G. Storz, J. Vogel and K. M. Wassarman, *Mol Cell*, 2011, 43, 880-891.
2. S. Gottesman and G. Storz, *Cold Spring Harb Perspect Biol*, 2011, 3, a003798.
3. D. Lalaouna, M. Simoneau-Roy, D. Lafontaine and E. Masse, *Biochim Biophys Acta*, 2013, 1829, 742-747.
4. R. G. Brennan and T. M. Link, *Curr Opin Microbiol*, 2007, 10, 125-133.
5. J. Vogel and B. F. Luisi, *Nat Rev Microbiol*, 2011, 9, 578-589.
6. D. Sledjeski and S. Gottesman, *Proc Natl Acad Sci U S A*, 1995, 92, 2003-2007.
7. F. Repoila and S. Gottesman, *J Bacteriol*, 2003, 185, 6609-6614.
8. N. Majdalani, C. Cunning, D. Sledjeski, T. Elliott and S. Gottesman, *Proc Natl Acad Sci U S A*, 1998, 95, 12462-12467.
9. R. A. Lease and S. A. Woodson, *J Mol Biol*, 2004, 344, 1211-1223.
10. W. Hwang, V. Arluison and S. Hohng, *Nucleic Acids Res*, 2011, 39, 5131-5139.
11. P. K. Brown, C. M. Dozois, C. A. Nickerson, A. Zuppardo, J. Terlonge and R. Curtiss, 3rd, *Mol Microbiol*, 2001, 41, 349-363.
12. A. Olsen, A. Arnqvist, M. Hammar, S. Sukupolvi and S. Normark, *Mol Microbiol*, 1993, 7, 523-536.
13. D. D. Sledjeski, A. Gupta and S. Gottesman, *Embo J*, 1996, 15, 3993-4000.
14. C. A. White-Ziegler, S. Um, N. M. Perez, A. L. Berns, A. J. Malhowski and S. Young, *Microbiology*, 2008, 154, 148-166.
15. R. A. Lease and M. Belfort, *Proc Natl Acad Sci U S A*, 2000, 97, 9919-9924.
16. P. Mandin and M. Guillier, *Curr Opin Microbiol*, 2013, 16, 125-132.

17. F. Repoila, N. Majdalani and S. Gottesman, *Mol Microbiol*, 2003, 48, 855-861.
18. P. Mandin and S. Gottesman, *EMBO J*, 2010, 29, 3094-3107.
19. K. M. Wassarman, F. Repoila, C. Rosenow, G. Storz and S. Gottesman, *Genes & Dev.*, 2001, 15, 1637-1651.
20. N. Zambrano, P. P. Guichard, Y. Bi, B. Cayrol, S. Marco and V. Arluison, *Cell Cycle*, 2009, 8, 2470-2472.
21. M. Vicente, A. I. Rico, R. Martinez-Arteaga and J. Mingorance, *J Bacteriol*, 2006, 188, 19-27.
22. F. Tetart and J. P. Bouche, *Mol Microbiol*, 1992, 6, 615-620.
23. A. Takada, M. Wachi and K. Nagai, *Biochem Biophys Res Commun*, 1999, 266, 579-583.
24. J. W. Shaevitz and Z. Gitai, *Cold Spring Harb Perspect Biol*, 2010, 2, a000364.
25. M. J. Osborn and L. Rothfield, *Curr Opin Microbiol*, 2007, 10, 606-610.
26. C. L. White and J. W. Guber, *Trends Microbiol*, 2012, 20, 74-79.
27. J. Dominguez-Escobar, A. Chastanet, A. H. Crevenna, V. Fromion, R. Wedlich-Soldner and R. Carballido-Lopez, *Science*, 2011, 333, 225-228.
28. H. Strahl, F. Burmann and L. W. Hamoen, *Nat Commun*, 2014, 5, 3442.
29. W. Margolin, *Curr Biol*, 2009, 19, R812-822.
30. M. Doi, M. Wachi, F. Ishino, S. Tomioka, M. Ito, Y. Sakagami, A. Suzuki and M. Matsuhashi, *J Bacteriol*, 1988, 170, 4619-4624.
31. M. Wachi, K. Osaka, T. Kohama, K. Sasaki, I. Ohtsu, N. Iwai, A. Takada and K. Nagai, *Biosci Biotechnol Biochem*, 2006, 70, 2712-2719.
32. R. Lange and R. Hengge-Aronis, *J Bacteriol*, 1991, 173, 4474-4481.

33. M. Aldea, C. Hernandez-Chico, A. G. de la Campa, S. R. Kushner and M. Vicente, *J Bacteriol*, 1988, 170, 5169-5176.
34. P. Freire, R. N. Moreira and C. M. Arraiano, *J Mol Biol*, 2009, 385, 1345-1351.
35. R. Guantes, B. Cayrol, F. Busi and V. Arluison, *Mol Biosyst*, 2012, 8, 1707-1715.
36. M. Wachi, M. Doi, S. Tamaki, W. Park, S. Nakajima-Iijima and M. Matsushashi, *J Bacteriol*, 1987, 169, 4935-4940.
37. A. R. Gruber, R. Lorenz, S. H. Bernhart, R. Neubock and I. L. Hofacker, *Nucleic Acids Res*, 2008, W70-W74.
38. F. Repoila and S. Gottesman, *J Bacteriol*, 2001, 183, 4012-4023.
39. C. A. McCullen, J. N. Benhammou, N. Majdalani and S. Gottesman, *J Bacteriol*, 2010, 192, 5559-5571.
40. I. Moll, T. Afonyushkin, O. Vytvytska, V. R. Kaberdin and U. Blasi, *Rna*, 2003, 9, 1308-1314.
41. H. Aiba, *Curr Opin Microbiol*, 2007, 10, 134-139.
42. A. Leroy, N. F. Vanzo, S. Sousa, M. Dreyfus and A. J. Carpousis, *Mol Microbiol*, 2002, 45, 1231-1243.
43. R. Hussein and H. N. Lim, *Nucleic Acids Res*, 2012, 40, 7269-7279.
44. A. Battesti, N. Majdalani and S. Gottesman, *Annu Rev Microbiol*, 2011, 65, 189-213.
45. J. M. Santos, P. Freire, M. Vicente and C. M. Arraiano, *Mol Microbiol*, 1999, 32, 789-798.
46. R. N. Moreira, C. Dressaire, S. Domingues and C. M. Arraiano, *Biochem Biophys Res Commun*, 2011, 411, 50-55.
47. N. De Lay, D. J. Schu and S. Gottesman, *J Biol Chem*, 2013, 288, 7996-8003.

48. T. Kruse, J. Moller-Jensen, A. Lobner-Olesen and K. Gerdes, *EMBO J*, 2003, 22, 5283-5292.
49. Y. Taniguchi, P. J. Choi, G. W. Li, H. Chen, M. Babu, J. Hearn, A. Emili and X. S. Xie, *Science*, 2010, 329, 533-538.
50. P. Mehta, S. Goyal and N. S. Wingreen, *Mol Syst Biol*, 2008, 4, 221.
51. Y. Shimoni, G. Friedlander, G. Hetzroni, G. Niv, S. Altuvia, O. Biham and H. Margalit, *Mol Syst Biol*, 2007, 3, 138.
52. J. Le Derout, I. V. Boni, P. Regnier and E. Hajnsdorf, *BMC Mol Biol*, 2010, 11, 17.
53. F. Geinguenaud, V. Calandrini, J. Teixeira, C. Mayer, J. Liquier, C. Lavelle and V. Arluison, *Phys Chem Chem Phys*, 2011, 13, 1222-1229.
54. T. Baba, T. Ara, M. Hasegawa, Y. Takai, Y. Okumura, M. Baba, K. A. Datsenko, M. Tomita, B. L. Wanner and H. Mori, *Mol Syst Biol*, 2006, 2, 2006 0008.
55. H. C. Tsui, G. Feng and M. E. Winkler, *J. Bacteriol.*, 1997, 179, 7476-7487.
56. L. M. Guzman, D. Belin, M. J. Carson and J. Beckwith, *J Bacteriol*, 1995, 177, 4121-4130.
57. R. Lutz and H. Bujard, *Nucleic Acids Res*, 1997, 25, 1203-1210.
58. J. H. Miller, in *A Laboratory Manual and Handbook for Escherichia coli and Related Bacteria*, ed. C. S. Harbor, Cold Spring Harbor Laboratory Press, NY, 1992/11/01 edn., 1992.
59. Y. L. Shih, I. Kawagishi and L. Rothfield, *Mol Microbiol*, 2005, 58, 917-928.
60. V. Girish and A. Vijayalakshmi, *Indian J Cancer*, 2004, 41, 47.
61. G. Pehau-Arnaudet, D. Joseleau-Petit and V. Arluison, *American Journal of Molecular and Cellular Biology*, 2012, 1, 17-24.
62. C. A. Schneider, W. S. Rasband and K. W. Eliceiri, *Nat Methods*, 2012, 9, 671-675.

63. T. Benaglia, D. Chauveau, D. R. Hunter and D. Young, *Journal of Statistical Software*, 2009, 32.
64. S. W. Chiu, S. Y. Chen and H. C. Wong, *Appl Environ Microbiol*, 2008, 74, 7016-7022.
65. R. A. Lease and M. Belfort, *Mol Microbiol*, 2000, 38, 667-672.
66. J. E. Cabrera and D. J. Jin, *J Bacteriol*, 2001, 183, 6126-6134.

Legends to the figures

Figure 1. Influence of stresses on MreB cellular concentration. Quantitative Western Blot using a purified anti-MreB antibody and total cell extracts of the indicated strains is presented as relative MreB levels. Wild type and mutants were grown to exponential phase at 37°C (black) and 16°C (grey), or to stationary phase at 37°C (empty). WT: DJ480; *dsrA*⁻: NM317 (DJ480Δ*dsrA*) and *hfq*⁻: DJ480 *hfq*::*cm*. Except otherwise indicated, the DJ480, NM317 and DJ480 *hfq*::*cm* were used. Standard deviation from 3 independent samples is shown in all experiments.

Figure 2. DsrA-mediated riboregulation on *mreB-lacZ* translational reporter fusion (Drawing is a schematic representation of the *mreB-lacZ* reporter fusion). Transcription of the plasmid encoded *mreB-lacZ* fusion is driven by P_{BAD} promoter in the presence of 0.001% L-arabinose. WT: DJ480/pNM12*mreB-lacZ*; *dsrA*⁻: DJ480Δ*dsrA*/pNM12*mreB-lacZ* and *hfq*⁻: DJ480 *hfq*::*cm*/pNM12*mreB-lacZ*. β-galactosidase activities in extracts from cells that were grown to exponential phase at 37°C (black) and 16°C (grey) or to stationary phase at 37°C (empty) are shown.

Figure 3. Model for the DsrA-MreB RNA duplex. The secondary structure model of *mreB*:DsrA complex was predicted by using RNAfold (<http://rna.tbi.univie.ac.at/cgi-bin/RNAfold.cgi>). *mreB* mRNA is shaded in grey and *mreB* Start codon (AUG) is highlighted. Note that the region of *mreB* pairing within DsrA includes part of the region used for pairing with *hns* and *rpoS*.^{8, 15}

Figure 4. DsrA regulates *mreB* expression through direct base pairing interaction. Comparison of β -galactosidase activities in extracts from DsrA⁻ cells (NM317) that expressed at 37°C plasmid encoded wild-type translation reporter fusion (*mreB*^{WT}-*lacZ*) or a mutant fusion (*mreB*^{mut}-*lacZ*) that carries mutations predicted to prevent annealing with wild-type DsrA (DsrA^{WT}). When indicated these cells also expressed plasmid encoded DsrA^{WT} or a DsrA mutant (DsrA^{mut}) that carries compensatory mutations predicted to restore annealing with *mreB*^{mut}-*lacZ*. Drawings are schematic representation of the *mreB*-*LacZ* reporter fusions (top) and the expected *mreB*-DsrA duplex RNAs (right). Transcription of both *lacZ* and DsrA derivatives is driven by P_{BAD} promoters in the presence of 0.002% L-arabinose. Observation of the activity and regulation required addition of twice as much inducer than in Figure 2, explaining thus the relatively higher activity. Shown strains from left to right: column 1 ($\Delta dsrA/P_{BAD}$ - *mreB*^{WT}-*lacZ*) ; column 2 ($\Delta dsrA/P_{BAD}$ - *mreB*^{WT}-*lacZ* + P_{BAD}- DsrA^{WT}) ; column 3 ($\Delta dsrA/P_{BAD}$ - *mreB*^{WT}-*lacZ* + P_{BAD}- DsrA^{mut}) ; column 4 ($\Delta dsrA/P_{BAD}$ - *mreB*^{mut}-*lacZ*) ; column 5 ($\Delta dsrA/P_{BAD}$ - *mreB*^{mut}-*lacZ* + P_{BAD}- DsrA^{mut}) ; column 6 ($\Delta dsrA/P_{BAD}$ - *mreB*^{mut}-*lacZ* + P_{BAD}- DsrA^{WT}).

Figure 5. Effect of DsrA on *mreB* mRNA concentration. Absolute quantifications of DsrA and *mreB* RNAs were performed by using reverse-transcription quantitative PCR (RT-qPCR)³⁵ and RNA extracted from wild type cells and mutants that lacked DsrA or Hfq. Cells were grown to exponential phase at 37°C and 16°C or stationary phase at 37°C. Levels of DsrA (grey) and *mreB* mRNA (black) are shown. ND: non detectable.

Figure 6. Effect of DsrA and Hfq on *mreB* mRNA half-life. Relative quantification of *mreB* mRNA were performed by RT-qPCR assay on RNA extracted from rifampicin-treated wild type

cells and mutants that lacked DsrA or Hfq. DJ480 *hfq::kan* was used for this analysis. Half-life of *mreB* mRNA from cells grown to exponential phase at 37°C (black) and 16°C (grey) is shown. Note that due to extremely low level of *mreB* mRNA under stationary phase (less than 1 copy per cell), accurate half-life measurement for this condition was not possible.

Figure 7. DsrA-mediated riboregulation changes the bacterial cell roundness under stress conditions. Cells were grown to reach exponential phase at 37°C and 16°C or stationary phase at 37°C then analyzed by measuring the long and short axis from cryo-TEM images. The statistics made on roundness (defined as the ratio between the shortest and longest axis of the cell computed from cryo-TEM images) for the different cell populations are summarized in the upper part of the figure. Examples of cells are shown in the lower part, with respective roundness indicated into parenthesis. Exp. Ph.: exponential phase of growth; St. Ph.: stationary phase of growth. WT: DJ480; DsrA⁻: NM317 (DJ480Δ*dsrA*) and DsrA⁻p-DsrA: DJ480Δ*dsrA*/*P_{BAD}-dsrA*. When indicated plasmid encoded DsrA was expressed in the presence of 0.001 % L-arabinose. *Scale bar 200 nm.*

Figure 8. Network of DsrA-dependent regulations. *mreB* was previously shown to be regulated at the transcriptional level by BolA transcription factor. As *bolA* gene is under the control of one main promoter driven by σ^S factor, its expression is itself dependent on sRNAs involved in *rpoS* post-transcriptional regulation in response to several stresses (DsrA, RprA, ArcZ and oxyS). Since the regulator and DNA organizer H-NS represses transcription of *bolA* and *rpoS*, DsrA also indirectly reduces the expression of *mreB* via repression of *hns* translation by DsrA (note that the nature of DsrA:*hns* complex is still unclear and that it has been proposed that the 3' UTR

of *hns* could be required for its post-transcriptional regulation).⁶⁵ Here we show that *mreB* translation is also directly repressed by the use of DsrA sRNA. sRNA regulators controlling mRNAs are depicted as rectangles and open arrows (X and Y, unidentified sRNAs); Hfq as a toroidal hexamer; σ^S , MreB and BolA proteins as grey ellipses, mRNAs as thick black lines; mRNA translation initiation region as a dark grey box; 5' and 3' of the mRNA are depicted by a “ball and arrow head”, respectively; transcriptional regulation are represented as thin grey lines; translational regulation as thin black lines; positive and negative regulation are indicated by arrows and horizontal bars, respectively; transcription promoters are indicated as P_x; dotted line symbolizes Peptidoglycan (PG) between outer (OM) and inner (IM) membranes.

Table 1 Strains and plasmids

Strain name	Description	Source
DJ480	MG1655 $\Delta lacX74$	66
NM317	DJ480 $\Delta dsrA$ (-10 to stem-loop 3 deletion)	8
DJ480 <i>hfq::kan</i>		This study
DJ480 <i>hfq::cm</i>		This study
AT171	MC1000 (<i>F- araD139</i> $\Delta(araABC-leu)7679$ <i>galU galK</i> $\Delta(lac)X74$ <i>rpsL thi</i>) $\Delta mreBCD$	This study

Plasmid name	Description	Origin/marker	Source
pNM12	Modified pBAD24 ⁵⁶ , to generate a promoter-less DNA fragment, <i>araC</i> , P _{BAD} , empty	ColE1/Amp ^R	8
pNM13	pNM12, <i>araC</i> , P _{BAD} , + DsrA insert	ColE1/Amp ^R	8
pBAD33-DsrA	Modified pBAD33 ⁵⁶ , <i>araC</i> , P _{BAD} , + DsrA insert	p15A/Cm ^R	This study
pBAD33-DsrA ^{mut}	Modified pBAD33DsrA, mutagenesis in <i>dsrA</i> sequence	p15A/Cm ^R	This study
pZE12-DsrA	Modified pZE12-MCS ⁵⁷ , P _{LacO-1} promoter, + DsrA insert	ColE1/Amp ^R	This study
pMec1 series	P _{mreB} ¹⁻²⁻³ , <i>mreB-lacZ</i> transcriptional and translational fusion	pSC101/Kan ^R	31
pNM12 <i>mreB-lacZ</i>	pNM12, <i>araC</i> , P _{BAD} , <i>mreB-lacZ</i> translational fusion	ColE1/Amp ^R	This study
pNM12 <i>mreB</i> ^{mut} - <i>lacZ</i>	Modified pNM12 <i>mreB-lacZ</i> ; mutagenesis in <i>mreB</i> 5' sequence	ColE1/Amp ^R	This study

Table 2 Primers used for qRT-PCR.

Gene name	Product size (bp)	Forward primer	Reverse primer
<i>dsrA</i>	69	CACATCAGATTTCTGGTGTAACG	GGGGTCGGGATGAAACTTGC
<i>mreB</i>	130	ACGGTGTGGTTTACTCCTCTTC	ATTTCGTGCTTGATACGTTCTG
<i>kan</i>	103	GCGAGTGATTTTGATGACGA	CATGAGTGACGACTGAATCC
<i>rrsB</i>	130	TGTCGTCAGCTCGTGTTGTG	ATCCCCACCTTCTCCAGTT

Table 3. Primers used for site-directed mutagenesis of *dsrA* and *mreB*.

Gene	Primer sequence (changed sequence is underlined)
<i>dsrA</i>	Forward: CAGATTTCTGGTGTT <u>GCTTAAAAAAGTTGTGCTTCTTGCTTAAG</u> Reverse: CTTAAGCAAGAAGC <u>ACA</u> ACTTTTTTAAGCAACACCAGGAAATCTG
<i>mreB</i>	Forward: GGATTATCCCTTAGTATGA <u>ATTTTTTTAAAGCAGGCATGTTTTCCAATG</u> Reverse: CATTGGAAAACATGCCT <u>GCTTTAAAAAAATT</u> CATACTAAGGGATAATCC

Table 4 Summary table.

	WT (DJ480)			$\Delta dsrA$			Δhfq		
	37°C	16°C	S. Ph.	37°C	16°C	S. Ph.	37°C	16°C	S. Ph.
MreB protein level (Relative Unit, %)	100±13	70±11	50±7	98±9	97±8	70±8	95±6	105±7	105±5
Translational fusion (Miller Unit)	405±33	425±124	55±25	380±60	900±160	95±41	805±90	800±65	95±41
<i>mreB</i> mRNA (Copy/cell)	9±1	4.5±0.5	0.3±0.12	8±0.5	5.5±0.8	0.5±0.15	3.5±0.5	3.5±0.5	ND
<i>mreB</i> mRNA half-life (min)	3.15±0.52	1.91±0.35	ND	2.23±0.52	6.41±0.12	ND	1.21±0.22	12±1.23	ND
Cell roundness (Percentage/roundness)	70%/0.36 30%/0.48	64%/0.37 36%/0.49	100%/0.59	87%/0.42 13%/0.65	100%/0.45	100%/0.50	ND	ND	ND

Fig. 1

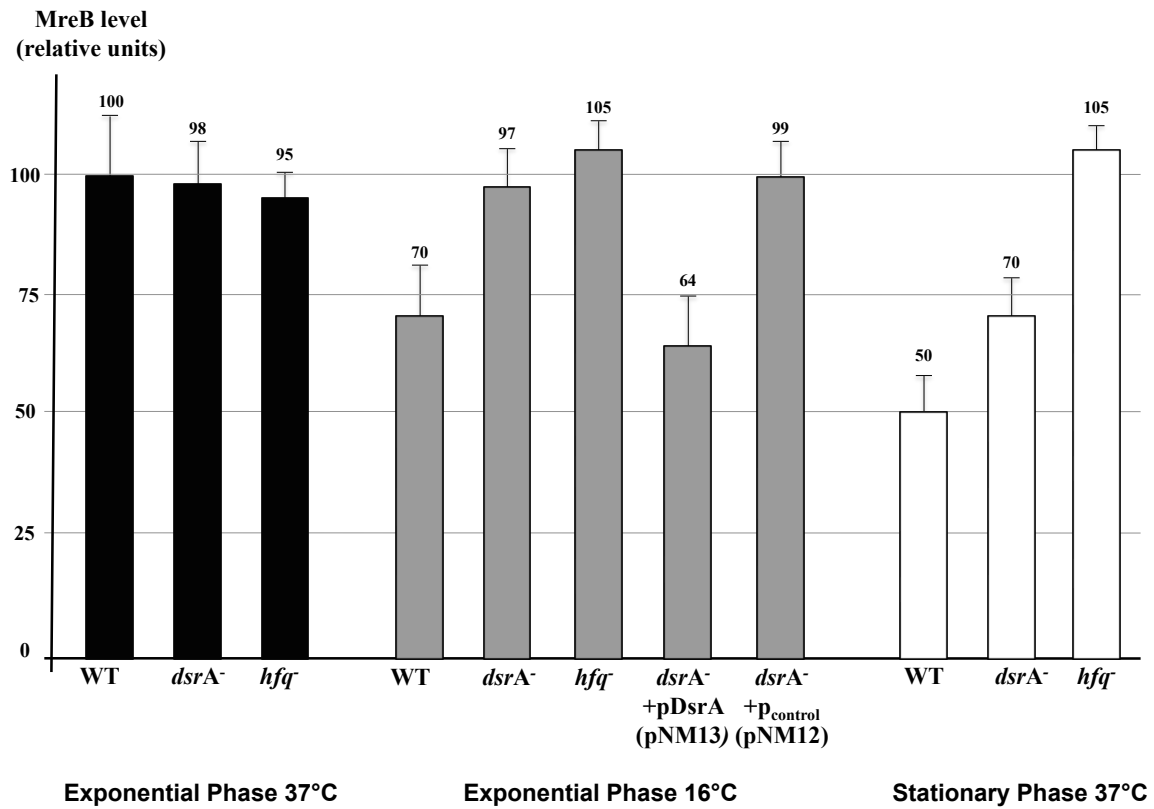


Fig. 2

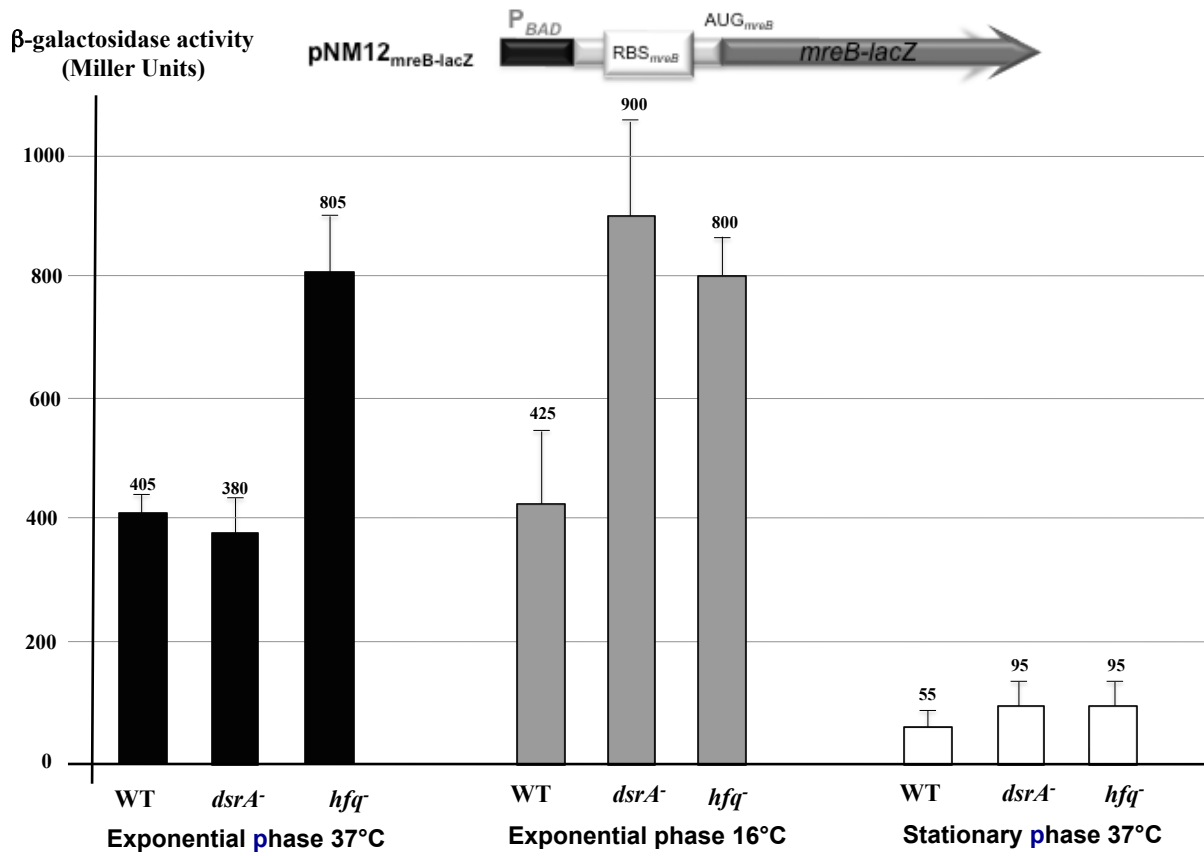


Fig. 4

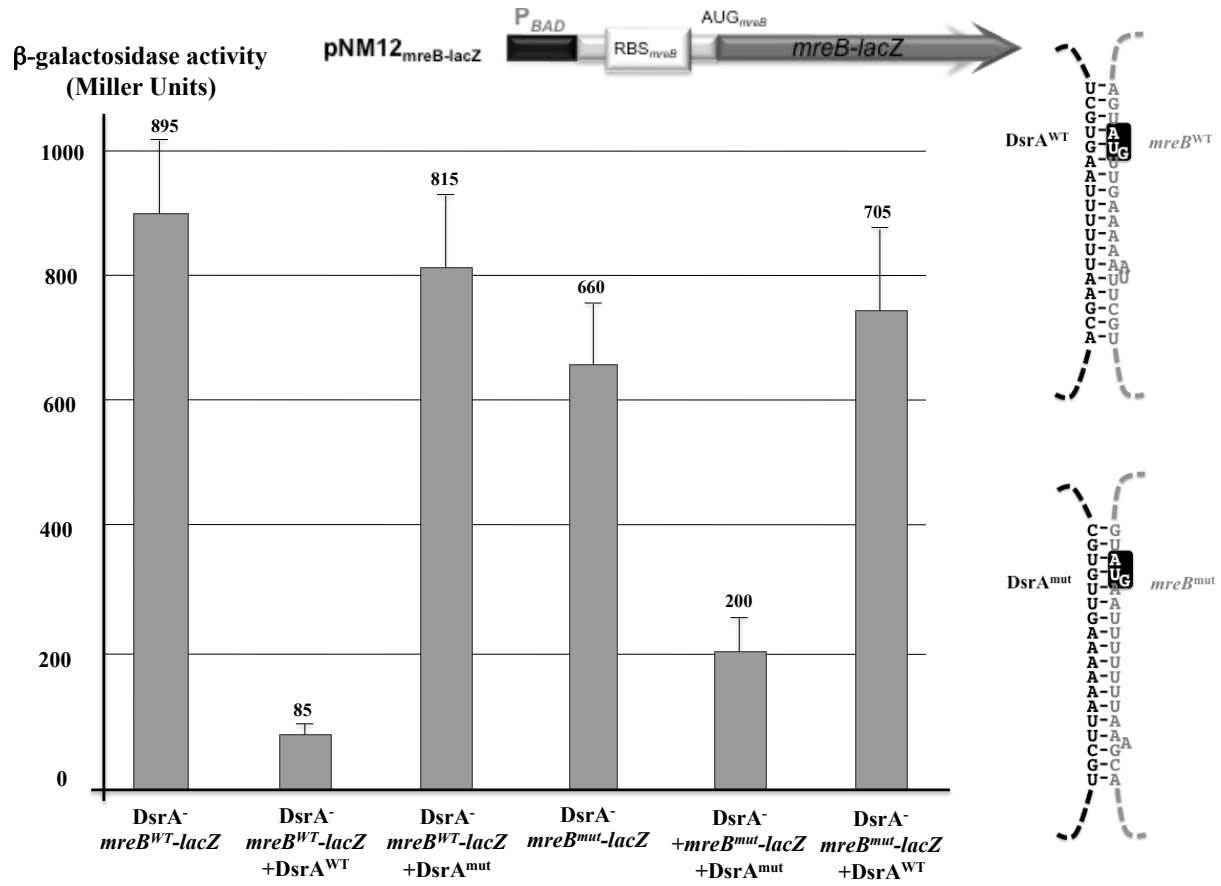


Fig. 5

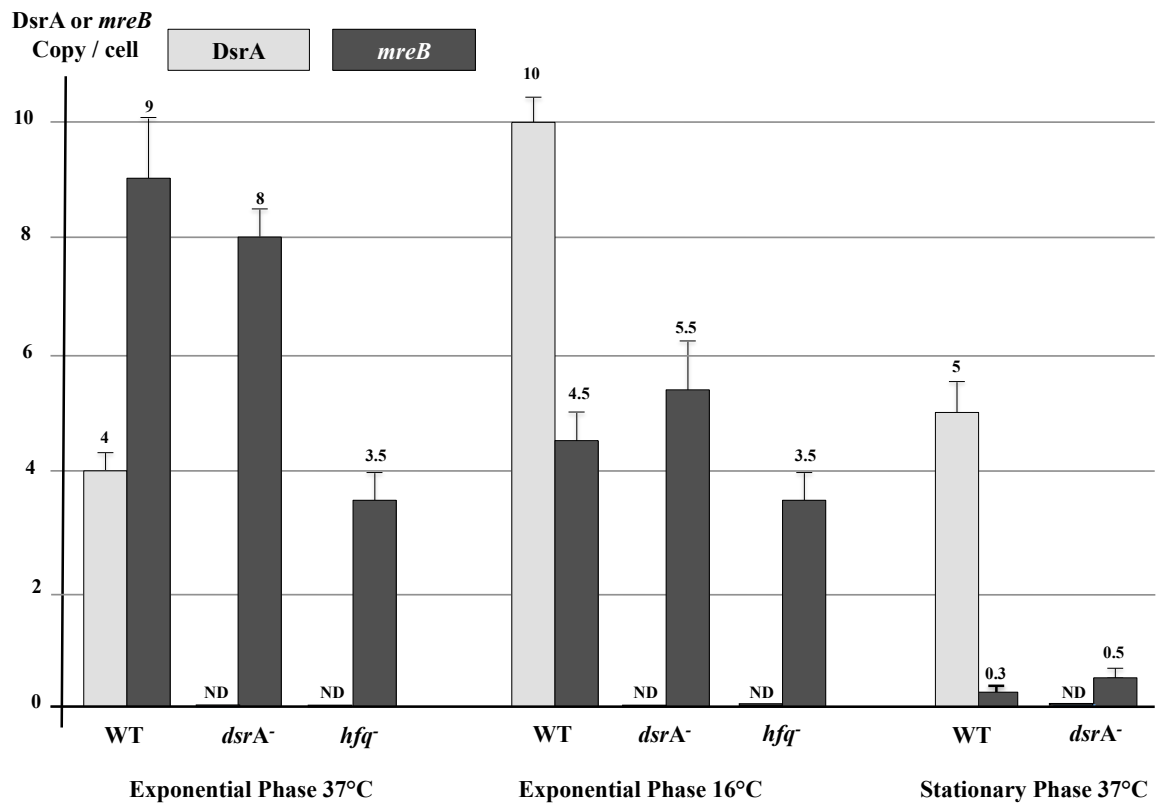


Fig. 6

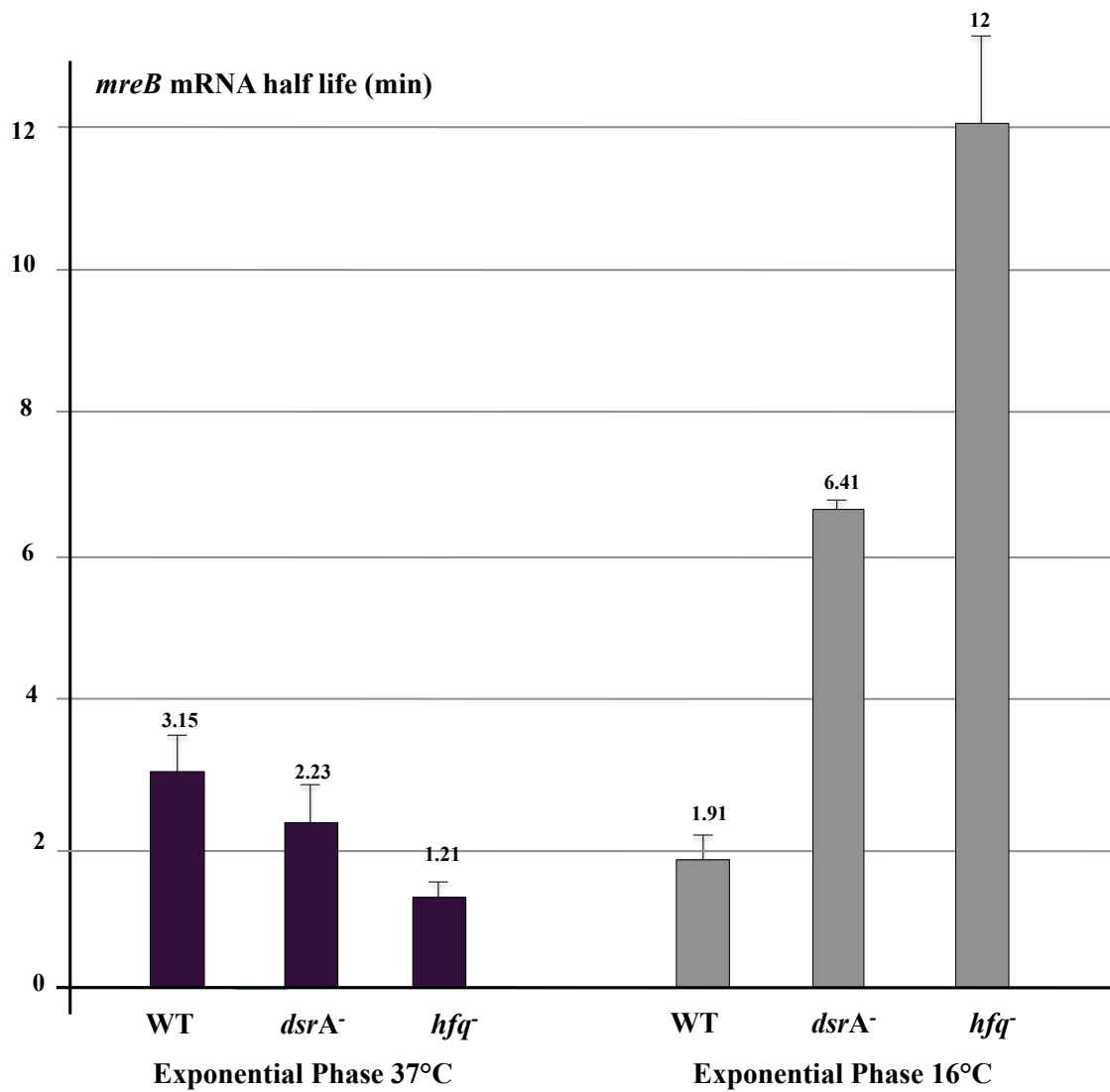
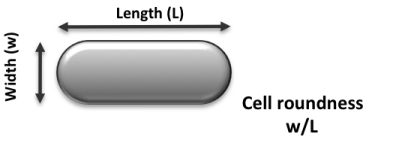
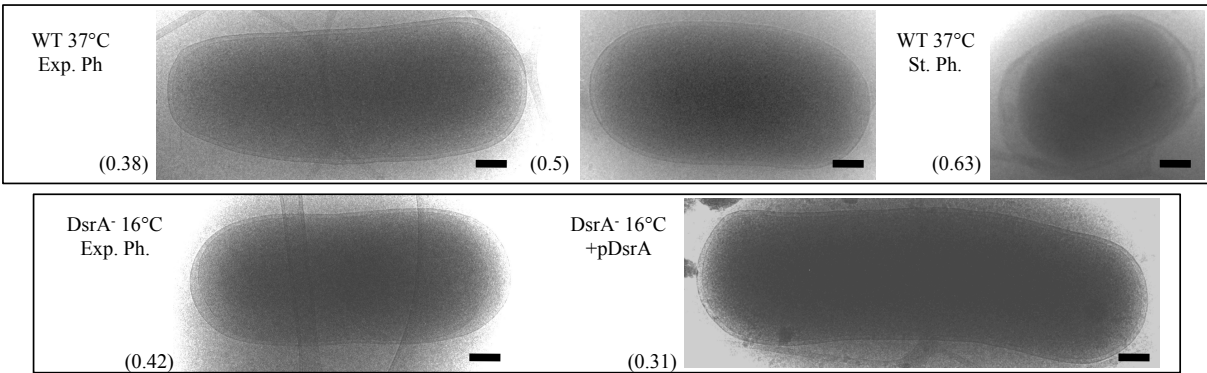


Fig. 7

		
WT 37°C Exp. Ph.	0.36 (70%)	0.48 (30%)
WT 16°C Exp. Ph.	0.37 (64%)	0.49 (36%)
DsrA ⁻ 37°C Exp. Ph.	0.42 (87%)	0.65 (13%)
DsrA ⁻ 16°C Exp. Ph.	0.45 (100%)	
WT St. Ph. 37°C	0.59 (100%)	
DsrA ⁻ St. Ph. 37°C	0.50 (100%)	
DsrA ⁻ 16°C Exp. Ph. + p-DsrA (pNM13)	0.33 (81%)	0.48 (19%)

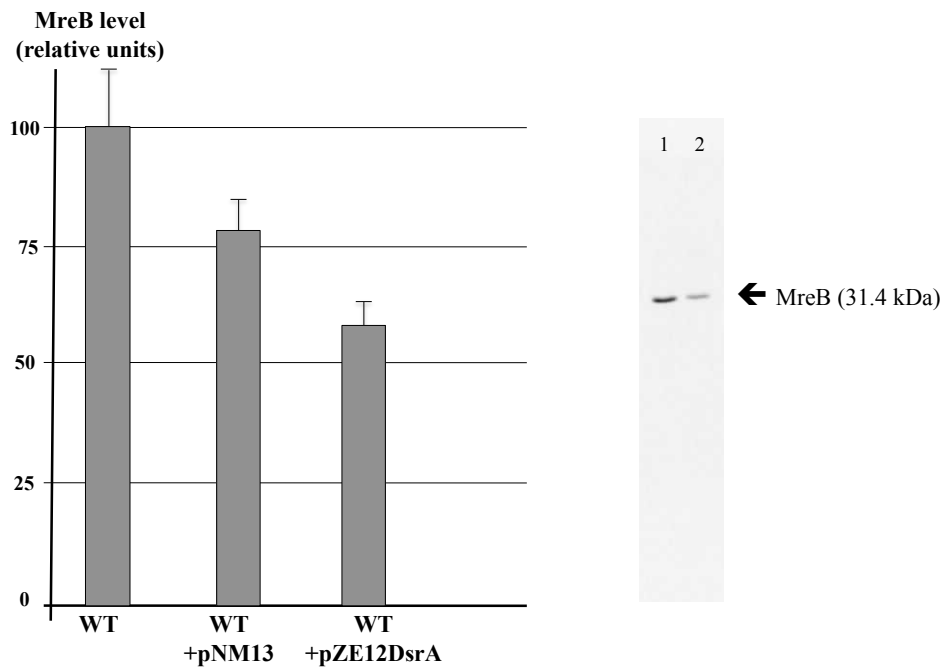


CCACTTGATACTAACGTGAAAAAATATTCACAAAGATACTCGGTT**TAAC**CTGCCGTTTAATCCGTTTTCCACTAGAC
 AT**AAATGCGCGCTGCGTCTCATGGGAGTGTGCTTGTCTGCTCGCCAGATTGTTGCAGCACATATGCAGATGAATGAC**
 P^{mreB}₃₋₁₀ -269
 CTTACGCGGTTGCAAACAGGCGAGGAATGCTGCTGATGCATTAAGCCTTTCT**TGGACT**CAGGCAGAGATT
 TGT**TAACAAA**GGAAACGAACTGCAC**TAATTTT**CACCGTAGCAGATGATTTTTGCGCCT**TGTC**GCTGCTGC
 P^{mreB}₂₋₁₀ -106 P^{mreB}₂₋₃₅ P^{mreB}₁₋₃₅
 GTGTGGTTGG**TAAAGT**AAGCGGATTTTCTTTTCCGCCCCAGCTTTCAGGATTATCCCT**AGTATGTTGA**
 P^{mreB}₁₋₁₀ -42 SD_{mreB} AUG_{mreB}
AAAAATTT**CGTGG**CATGTTTTCCAATGACTTGTCCATTGACCTGGGTACTGCGAATACCCTCATTATG
 TAAAAGGACAAGGCATCGTATTGAATGAGCCTTCCGTGGTGGCCATTCGTCAGGATCGTGCCGGTTCCAC
 CGAAAAGCGTAGCTGCAGTAGGTCATGACGCGAAGCAGATGCTGGGCCGTACGCCGGGCAATATTGCTG
 CCATTCGCCCAATGAAAGACGGCGTTATCGCCGACTTCTTCGTGACTGAAAAAATGCTCCAGCACTTCA
 TCAAACAAGTGCACAGCAACAGCTTTATGCGTCCAAGCCGCGGTTCTGGTTTTGTGTGCCGGTTGGCG
 CGACCCAGGTTGAACGCCGCGCAATTTCGTGAATCCGCGCAGGGCGCTGGTGCCCGTGAAGTCTTCTCTGA
 TTGAAGAACCGATGGCTGCCGCAATTGGTGTGGCCTGCCGTTTCTGAAGCGACCGGTTCTATGGTGG
 TTGATATCGGTGGTGGTACCCTGAAGTTGCTGTTATCTCCTTGAACGGTGTGGTTACTCCTCTTCTG
 TGCGCATTGGTGGTGACCGTTTTCGACGAAGCTATCATCAACTATGTGCGTCGTAATTACGGTTCTCTGA
 TCGGTGAAGCCACCGCAGAACGTATCAAGCACGAAATCGGTTTCGGCTTATCCGGGCGATGAAGTCCGTG
 AAAATCGAAGTTTCGTGGCCGTAACCTGGCAGAAGGTGTTCCACGCGGTTTTACCCTGAACTCCAATGAAA
 TCCTCGAAGCACTGCAGGAACCGCTGACCGGTATTGTGAGCGCGGTAATGGTTGCACTGGAACAGTGCC
 CGCCGGAACCTGGCTTCCGACATCTCCGAGCGCGCATGGTGTCCACCGGTGGTGCGCACTGCTGCGTA
 ACCTTGACCGTTTGTTAATGGAAGAAACCGGCATTCAGTCGTTGTTGCTGAAGACCCGCTGACCTGTG
 TGGCGCGCGGTGGCGGCAAAGCGCTGGAAATGATCGACATGCACGGCGCGACCTGTT**CAGCGAAGAGT**
 A**AT**TCGGATGCAGGCAGGGGAAGTGTCTGTTACCCTGCCTGGTCTGATACGAGAATACGCATAACT**ATGAAGCCA**
 mreB stop AUG_{mreC}
 ATTTTTAGCCGTGGCCCGT**CGCTACAGATTCGCCTTATTCTGGCGGTGCTG...**
 mreC coding sequence

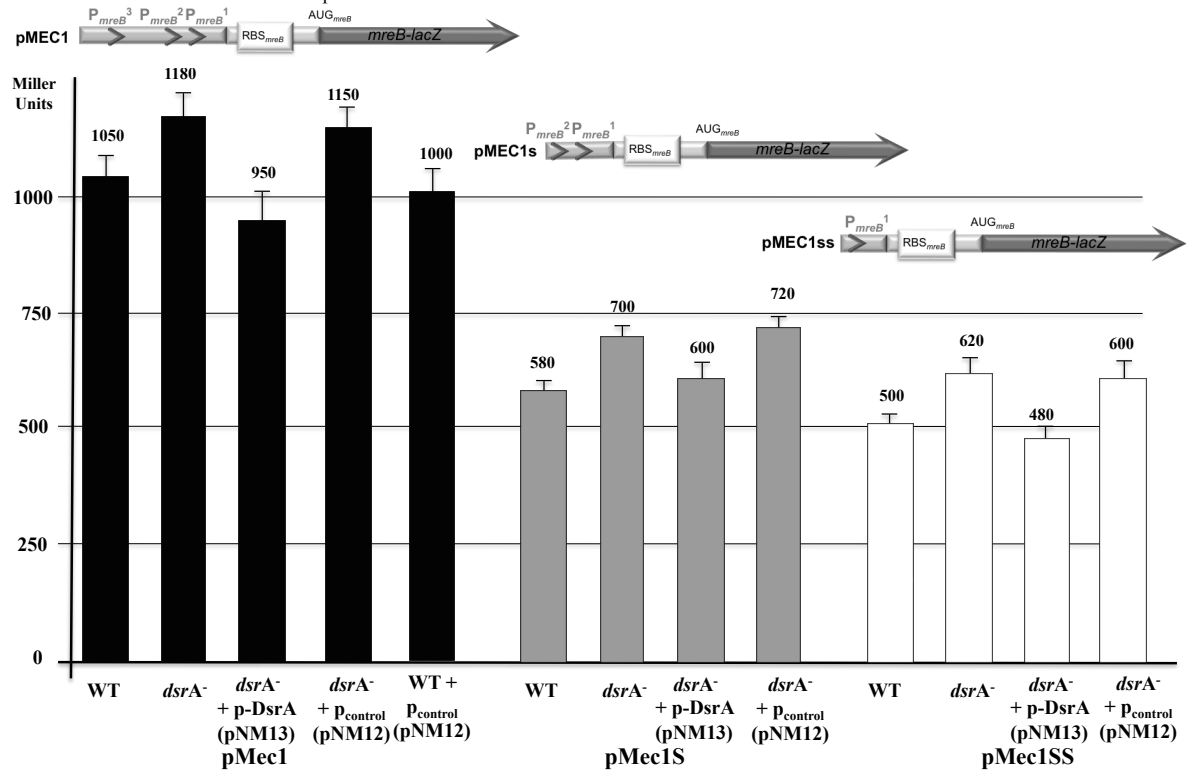
Supplementary figure S1: DNA sequence of *mreB* region. The *mreBCD* region is located at ~ 73 min in the *E. coli* chromosome.¹ Three σ^D -dependent promoters contribute to *mreB* transcription (P^{mreB}₁, P^{mreB}₂ and P^{mreB}₃, -10 and -35 boxes) and are indicated as black boxes. Probable transcription initiation sites (-269, -106 and -42) are indicated in bold.² Note that -106 initiation site is atypical and could in fact result from a post-transcriptional cleavage by an RNase.² Shine Dalgarno (SD) and translation initiation codon of *mreB* are indicated. The region of *mreB* that anneals with DsrA is underlined with a wavy line. The coding sequence of *mreB* is indicated in light grey, whereas the beginning of *mreC* coding sequence appears in dark grey. Stop codon of *mreB* and *yhdA* upstream gene (located nearby P^{mreB}₃, -35)³ are italicized.

1. M. Doi, M. Wachi, F. Ishino, S. Tomioka, M. Ito, Y. Sakagami, A. Suzuki and M. Matsushashi, *J Bacteriol*, 1988, 170, 4619-4624.
2. M. Wachi, K. Osaka, T. Kohama, K. Sasaki, I. Ohtsu, N. Iwai, A. Takada and K. Nagai, *Biosci Biotechnol Biochem*, 2006, 70, 2712-2719.
3. N. Sommerfeldt, A. Possling, G. Becker, C. Pesavento, N. Tschowri and R. Hengge, *Microbiology*, 2009, 155, 1318-1331.

Supplementary figure S2: Influence of DsrA on MreB concentration. *Left panel:* MreB quantifications were made by Western Blot as described in methods and Fig.1. Two plasmids allowing the expression of DsrA under the control of P_{BAD} (pNM13 + 0.01% arabinose) and constitutive P_{LacO-1} (pZE12) promoters were used. Both plasmids resulted in a significant diminution of MreB levels. *Right panel:* an example of Western Blot using a cell extract in the presence (*lane 2*) or not (*lane 1*) of a plasmid that express DsrA (constitutive expression). As shown, anti-MreB antibody is specific.



Supplementary figure S3: DsrA-mediated riboregulation on *mreB-lacZ* translational and transcriptional reporter fusion. β -galactosidase activities were assayed in cell extracts of the indicated strains grown at 16°C (exponential phase). Drawing is a schematic representation of the *mreB-lacZ* reporter fusion. We observe that DsrA affects *mreB* expression and that DsrA expression from pNM13 (+ 0.001% L-arabinose) in a Δ *dsrA* background complements *dsrA* phenotype, while the empty pNM12 vector does not. Note that the effect observed for Δ *dsrA* strain is slightly less than that seen for the protein level (Fig. 1). Nevertheless, fusion reflects *mreB-lacZ* RNA and MreB-lacZ protein stabilities, which is different from *mreB* mRNA and MreB protein stabilities.



Supplementary figure S4: The secondary structure model of *mreB*:DsrA complexes predicted using RNAfold server (<http://rna.tbi.univie.ac.at/cgi-bin/RNAfold.cgi>). The *mreB* AUG start codon is highlighted. Both WT and mutated *mreB* and DsrA pairings are shown.

